A small membrane protein critical to both the offensive and defensive capabilities of *Staphylococcus aureus.*

Seána Duggan[1#], Maisem Laabei[2#], Alaa Alnahari[1], Eóin C. O'Brien[3], Keenan A. Lacey[3$], Leann Bacon[1], Kate Heesom[4], Chih-Lung Fu[5], Michael Otto[5], Eric Skaar[6], Rachel M. McLoughlin[3] and Ruth C. Massey[1*]

1: School of Cellular and Molecular Medicine, University of Bristol, Bristol, UK.

2: Department of Biology and Biochemistry, University of Bath, Bath, UK.

3: Host-Pathogen Interactions Group, School of Biochemistry and Immunology, Trinity Biomedical Sciences Institute, Trinity College Dublin, Ireland.

4: University of Bristol Proteomics Facility, Biomedical Sciences Building, University Walk, Bristol, BS8 1TD, UK.

5: Pathogen Molecular Genetics Section, Laboratory of Bacteriology, National Institute of Allergy and Infectious Diseases, U.S. National Institutes of Health, Bethesda, Maryland, USA.

6: Department of Pathology, Microbiology, and Immunology, Vanderbilt University Medical Center, Nashville, TN, USA.

$: Current Address: Department of Microbiology, New York University School of Medicine, New York, NY 10016, USA.

[#] contributed equally to this work

* for correspondence: ruth.massey@bristol.ac.uk

Abstract

Staphylococcus aureus is a major human pathogen, where the widespread emergence of antibiotic resistance is making infections more challenging to treat. Toxin induced tissue damage and resistance to the host's immune system are well established as critical to its ability to cause disease. However, recent attempts to study *S. aureus* pathogenicity at a population level have revealed significant complexity and hierarchical levels of regulation. In an effort to better understand this we have identified and characterized a principle effector protein, MasA. The inactivation of this small highly-conserved membrane protein simultaneously disrupts toxin production and impairs *S. aureus'* ability to resist several aspects of the innate immune system. These pleiotropic effects are mediated by both a change in the stability of the bacterial membrane and the dysregulation of iron homeostasis, which results in a significant impairment in the ability of *S. aureus* to cause infection in both a subcutaneous and a sepsis model of infection. That proteins with such major effects on pathogenicity remain unidentified in a bacterium as well studied as *S. aureus* demonstrates how incomplete our understanding of their ability to cause disease is, an issue that needs to be addressed if effective control and treatment strategies are to be developed.

Introduction

Staphylococcus aureus is a major human pathogen, where the types of infections it causes range in severity from relatively superficial skin and soft tissue infections (SSTIs) to fatal cases of endocarditis and bacteraemia[1,2]. While SSTIs rarely require clinical intervention, more invasive or prolonged infections require antibiotic treatment. Unfortunately, the widespread use of antibiotics has given rise to the emergence of antibiotic resistant strains of *S. aureus*, including the notorious methicillin resistant *S. aureus* (MRSA), which at its peak was reported to be responsible for in excess of 50% of *S. aureus* infections in hospitals[3]. Infection control measures and changes to antibiotic usage policies have led to a decrease in the incidence of MRSA in several counties. In England, where the surveillance of *S. aureus* bacteraemia is mandatory, the incidence of MRSA declined for several years (by >80% since 2007) and has recently plateaued[4]. However, the incidence of methicillin sensitive *S. aureus* (MSSA) bacteraemia has increased year on year and is now 29.4% higher than it was in 2011 when mandatory surveillance began[3], a worrying trend that has also been observed in other countries[4,5]. Although new classes of antibiotics are under development, given the rate at which *S. aureus* evolves resistance, it is clear that we need to improve our understanding of this pathogen to develop alternative therapeutic strategies.

To date, our understanding of *S. aureus* pathogenicity has largely been informed by the analysis of a small number of laboratory strains that have been passaged *in vitro* many times. This approach has enabled the identification and characterisation of many of the proteins used by *S. aureus* to cause disease, and some of the complex means by which it regulates the expression of these proteins. For example, the secretion of toxins such as alpha-toxin[6,7] and the phenol-soluble modulins (PSMs)[7,8] has been associated with increased virulence; and nearly all toxins are under the control of a two-component, quorum sensing system called the accessory gene regulator (Agr)[9,10]. However, many additional regulatory systems also contribute to *S. aureus* virulence e.g. the alternative sigma factor, SigB, which amongst other things governs the characteristic gold pigmentation of *S. aureus*, a result of the expression of

the carotenoid staphyloxanthin[11]. Without this the bacteria are less able to defend themselves from immune attack. Not only is there huge diversity and complexity to the means by which *S. aureus* interacts with its host to cause disease, recent work suggests that clones might utilise distinct pathways to achieve this[12]. With such complexity and functional redundancy, this may explain why efforts to develop interventions, such as a protective vaccine, have not yet been successful.

To better understand the pathogenicity of *S. aureus*, we developed a functional genomics approach to make use of the many thousands of clinical *S. aureus* isolates that have been sequenced[12-14]. This has enabled us to identify novel loci that affect the ability of *S. aureus* to both secrete cytolytic toxins and form biofilm[12-14]. One locus we found to be associated with the ability of the bacteria to secrete toxins was annotated as a putative membrane bound protein. Here we characterised the *in vitro* and *in vivo* properties of this protein, which we name MasA, demonstrating its pleiotropic effects on many established *S. aureus* activities including toxin production and resistance to innate immune mechanisms. We show that *masA* disruption results in membrane instability and dysregulation of iron homeostasis, which subsequently has a crippling effect on virulence and enhanced clearance in both a subcutaneous and a systemic model of infection. Given how well studied *S. aureus* is, that a locus with such a dominant effect on pathogenicity has remained until now undiscovered is somewhat surprising. A feature that is further compounded by the fact that there are homologues of this protein in many other human pathogens, including some as distantly related as the *Vibrio* genus, which suggests that defining the activity of this protein could have widespread implications for the understanding of the virulence of many bacterial pathogens.

RESULTS

The MasA protein positively affects the production of cytolytic toxins by *S. aureus*.

In previous work we found an association between a gene with the locus tag SATW20_23930 in the TW20 MRSA background and the ability of clinical strains to lyse human cells[13]. We have named the gene *masA* for membrane active stabiliser, as our data (presented later) suggest it plays a critical role in the membrane stability of the bacteria. With the availability of a transposon library in the USA300 MRSA background, we sought this gene and found that it was mis-annotated in the FPR3757 background as intergenic between SAUSA300_2212 and SAUSA300_2213[15]. We were however able to obtain transposon mutants in this region from the Nebraska Transposon Mutant Library[16], where we found that inactivation of this gene reduced the ability of the bacteria to lyse THP-1 cells, which is an immortalised cell line that is sensitive to the majority of the cytolytic toxins expressed by *S. aureus*[13,14] (Fig. 1A). This effect on toxicity was complemented by expressing the *masA* gene from an inducible promoter on the pRMC2 plasmid[17] (Fig. 1A). To confirm the effect was not specific to this genetic background we transduced the transposon insertion into a genetically distinct methicillin sensitive *S. aureus* (MSSA) strain, SH1000[18], where again it resulted in the loss of cytolytic activity for the bacteria (fig. 1B). The effect on toxicity was further confirmed on A549 cells (Fig. 1C) and human red blood corpuscles (Fig. 1D) which contain the additional receptors for alpha toxin and PVL, demonstrating the widespread effect the loss of this protein has on cytolytic toxin secretion by both MRSA and MSSA.

We next quantified the effect the inactivation of MasA has on the expression of several toxins to confirm whether its activity was specific to a single *S. aureus* toxin or had a more general effect. In both the JE2 and SH1000 background the inactivation of *masA* resulted in a decrease in alpha toxin secretion as demonstrated by western blotting of bacterial supernatant (Fig. 1E and Supplementary Fig. 1). There is also a reduction in the secretion of several of the phenol soluble modulins, including delta toxin which was determined by HPLC-MS (Fig. 1F). For both alpha toxin and the PSMs the effect of the inactivation of *masA* was more pronounced

in the SH1000 background. Given the effect on the production of all these toxins we hypothesised that the effect of the inactivation of *masA* could be mediated by repression or lack of activation of the major regulator of toxin expression, the accessory gene regulatory (Agr) quorum sensing system. To test this, we quantified the transcription of the regulatory RNA effector molecule of the Agr system, *rnaIII*, and found this to be significantly lower in the *masA* mutants, explaining the effect on toxicity we have observed (Fig. 1G).

To better understand the activity of this gene we examined both its genomic location and the likely cellular location of the encoded protein. The *masA* gene is situated between a hypothetical protein and an AcrB/AcrD/AcrF family protein (Supplementary Fig. 2A). To examine the role of the genes located to either side of the *masA* gene (Fig. 1A), we quantified the toxicity of transposon mutants in these genes in both the JE2 USA300 MRSA and SH1000 MSSA backgrounds, and found there to be no effect, with the exception of a slight reduction in toxicity for NE42 (SAUSA300_2212) in the JE2 background (Supplementary Fig. 2B). We also performed western blots to quantify alpha toxin production and extracted the PSMs from culture supernatants (Supplementary Fig. 2C and D) and found these activities were only affected in the *masA* mutant, suggesting that the genes to either side of *masA* play a minimal role in the effect of MasA on cytolytic toxin production. To understand the potential cellular localisation of the translated protein, we used the protein structure predicting software Protter[19], which suggests that MasA is a membrane bound protein with four transmembrane domains, both the C and N terminus are predicted to be exposed to the outside on the membrane and it lacks a recognised signal sequence (Fig. 1H).

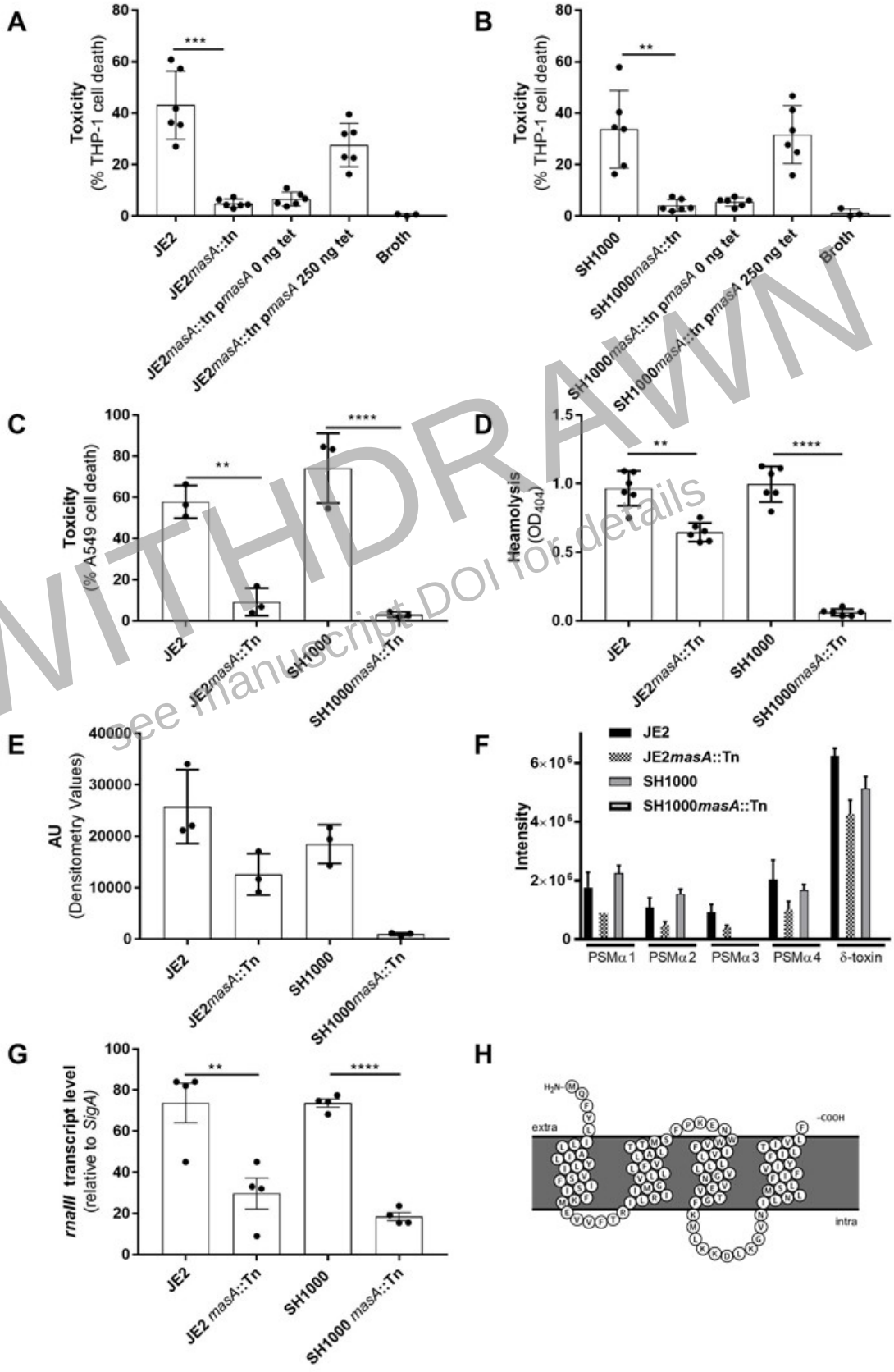

150

151 **Figure 1**

Inactivation of the *masA* gene results in a loss of toxicity (cytolytic activity) for *S. aureus*. In both the JE2 (**A**) and SH1000 (**B**) backgrounds the inactivation of *masA* resulted in a loss of cytolytic activity represented by a significant decrease in cell death. The loss of cytolytic activity was complemented in both backgrounds by expressing the *masA* gene from a plasmid (p*masA*) (**A** and **B**). Furthermore, the inactivation of *masA* resulted in a loss of toxicity to a lung epithelial cell line (A549) (**C**) and human red blood corpuscles (**D**) in both the JE2 and SH1000 backgrounds. Inactivation of *masA* also resulted in a reduction in alpha toxin secretion in both backgrounds, determined by Western blot. Densitometry values for triplicate blots are shown (**E**). (**F**) The effect of the inactivation of *masA* on secretion of PSMs was quantified by HPLC, where the secretion of delta toxin was the most affected in both backgrounds ($p<0.001$). (**G**) The activity of the Agr system is repressed by the inactivation of *masA* as illustrated by qRT-PCR quantification of *rnaIII* transcription. Statistics were performed using the Student's paired *t*-test and significance was determined as < *0.05; **0.01; ***0.001.

The MasA protein contributes to the ability of *S. aureus* to protect itself from the innate immune system.

As we worked with the *masA* mutant strains, we observed the colonies were less golden in colour than either wild type strain. This characteristic colour for *S. aureus* is a result of the production of a carotenoid pigment called staphyloxanthin, which has been shown to play a role in the intra-cellular survival of the bacteria[20] as well as contributing the membrane rigidity and the ability of the bacteria to protect themselves from elements of the innate immune system such as antimicrobial peptides and fatty acids[21]. We quantified staphyloxanthin production and found that in both *S. aureus* backgrounds the *masA* mutants produce significantly less of this protective pigment (Fig. 2A).

To examine whether this loss in staphyloxanthin production was sufficient to affect the ability of the bacteria to defend itself from aspects of the innate immune system, we quantified the ability of the bacteria to withstand the membrane damaging effects of human defensin-1 and oleic acid. The inactivation of *masA* in both *S. aureus* backgrounds significantly impaired their ability to survive exposure to these elements (Fig. 2B and C). To examine whether this was due to a difference in the stability of lipid bilayer we also examined the sensitivity of the bacteria to the surfactant activity of sodium dodecyl sulphate (SDS), where again we found that the mutants were significantly impaired in protecting themselves (Fig. 2D). As staphyloxanthin has also been shown to confer protection to *S. aureus* during phagocytosis,

187 we investigated the bacteria's ability to survive inside macrophages (PMA differentiated THP-
188 1 cells) (Fig. 2E) and human blood (Fig. 2F). In both *S. aureus* backgrounds the mutant
189 survived less well than the wild type strains. As membrane integrity has also been attributed
190 to staphyloxanthin[21], we determined whether this was also affected in the MasA mutants.
191 Bacteria were cultured overnight and stained with propidium iodide (PI) to assess membrane
192 integrity via FACS (Fig. 2G and H). The shift in PI staining for the *masA* mutants indicates a
193 reduced membrane integrity compared to the wild type strains. As such it is clear that in
194 addition to the contribution MasA makes to toxin production, it also contributes to membrane
195 integrity and the ability of the bacteria to protect itself from the host's immune response.
196

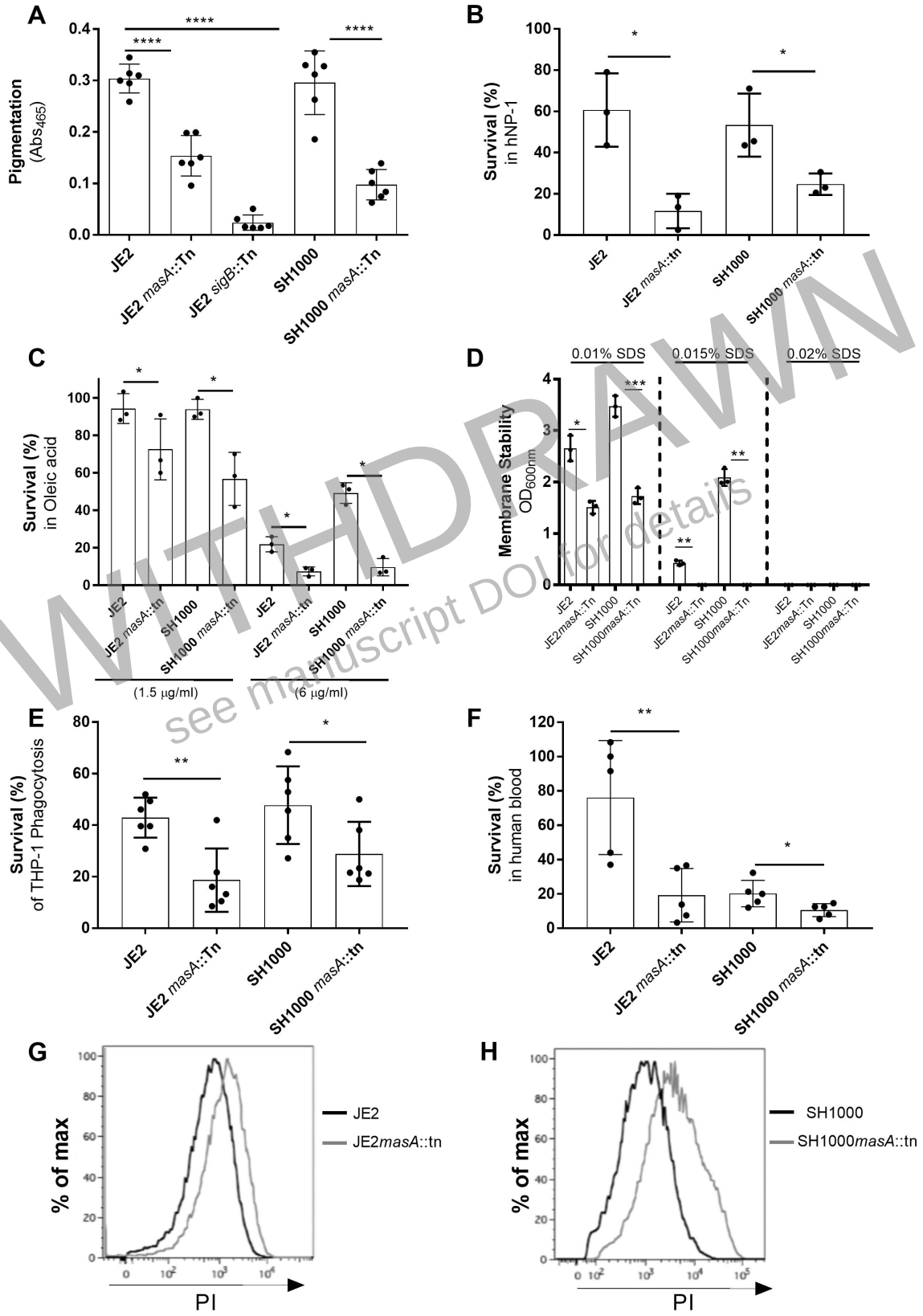

197

198 **Figure 2**
199 MasA confers protection against aspects of innate immunity (**A**) Inactivation of *masA* results
200 in decreased staphyloxanthin production in both *S. aureus* backgrounds. (**B**) Survival of *S.*
201 *aureus* upon exposure to the human neutrophil defensin-1 (hNP-1) was reduced in the *masA*

mutants in both *S. aureus* backgrounds. (**C**) Survival of *S. aureus* upon exposure to oleic acid was reduced in the *masA* mutants in both *S. aureus* backgrounds. (D) Survival of *S. aureus* upon exposure to SDS was reduced in the *mas*A mutants in both *S. aureus* backgrounds. (**E**) Survival of *S. aureus* following phagocytosis is reduced in the *mas*A mutants in both *S. aureus* backgrounds. (**F**) Survival in human blood is reduced in the absence of *masA* in both backgrounds. (**G** and **H**) FACS analysis of wild type and *masA* mutants in both backgrounds stained with propidium iodide (PI) demonstrates a decrease in membrane integrity in the *masA* mutants. Statistics were performed using one-way ANOVA or the Student's paired *t*-test and significance was determined as < *0.05; **0.01; ***0.001; ****0.0001.

The loss of MasA significantly attenuates the ability of *S. aureus* to cause disease.

The loss of the Agr system has been shown in several models of infection to attenuate the pathogenicity of *S. aureus*. However, the MasA mutants are not only impaired in the activation of the Agr system they are also less able to protect themselves from host immunity. To examine the effect the loss of both offensive and defensive capabilities has *in vivo*, we utilised a murine subcutaneous infection model and compared the *masA* mutant to both the wild type JE2 strain and an *agrB* mutant. Photographs of the appearance of the abscesses were captured daily (Fig. 3A), and both the bacterial density in skin punch biopsies (Fig. 3B) and the abscess lesion area (Fig. 3C) were compared for all three strains. As demonstrated previously[10], the loss of the Agr system significantly attenuates the ability of *S. aureus* to cause infection. However, the *masA* mutant was significantly more attenuated than the *agrB* mutant in terms of both abscess lesion area and tissue bacterial burden in our murine subcutaneous infection model, demonstrating the considerable effect the loss of both toxicity and immune evasion capacities have on pathogenicity *in vivo*.

Given the importance of both toxin production and immune defence during invasive infection we also compared the pathogenicity of the *masA* mutant in sub-lethal murine sepsis model. Six and 24hrs after tail vein inoculation the density of bacteria in blood, kidneys and spleen were quantified. In blood after 6 hours both the *agrB* and *masA* mutants were more effectively cleared compared to the wild type strain, and by 24hrs all three strains were barely detectable (Fig. 3D). In both the spleens and livers at both six and 24 hours post infection the wild type strain was more abundant, and comparable bacterial burdens were detected for the *masA* and

agrB mutant strains (Fig. 3E, F). In the kidneys at 6hrs post infection both the wild type and *agr* mutant were present at similar levels, however we were unable to detect any *masA* mutant cells. By 24hr in the kindeys we were able to detect the *masA* mutant and they were at an equivalent burden when compared to the *agr* mutant, however both mutants were at a significantly lower level when compared to the wild type strain (Fig. 3G). This suggest that both mutant were impaired in their ability to establish an infection in the kidney, where the *masA* mutant appears to have a greater impairment in its ability to disseminate to the kidneys during the early stages of infection, possibly as a result of its increased sensitivity to the membrane attacking elements of the innate immune system.

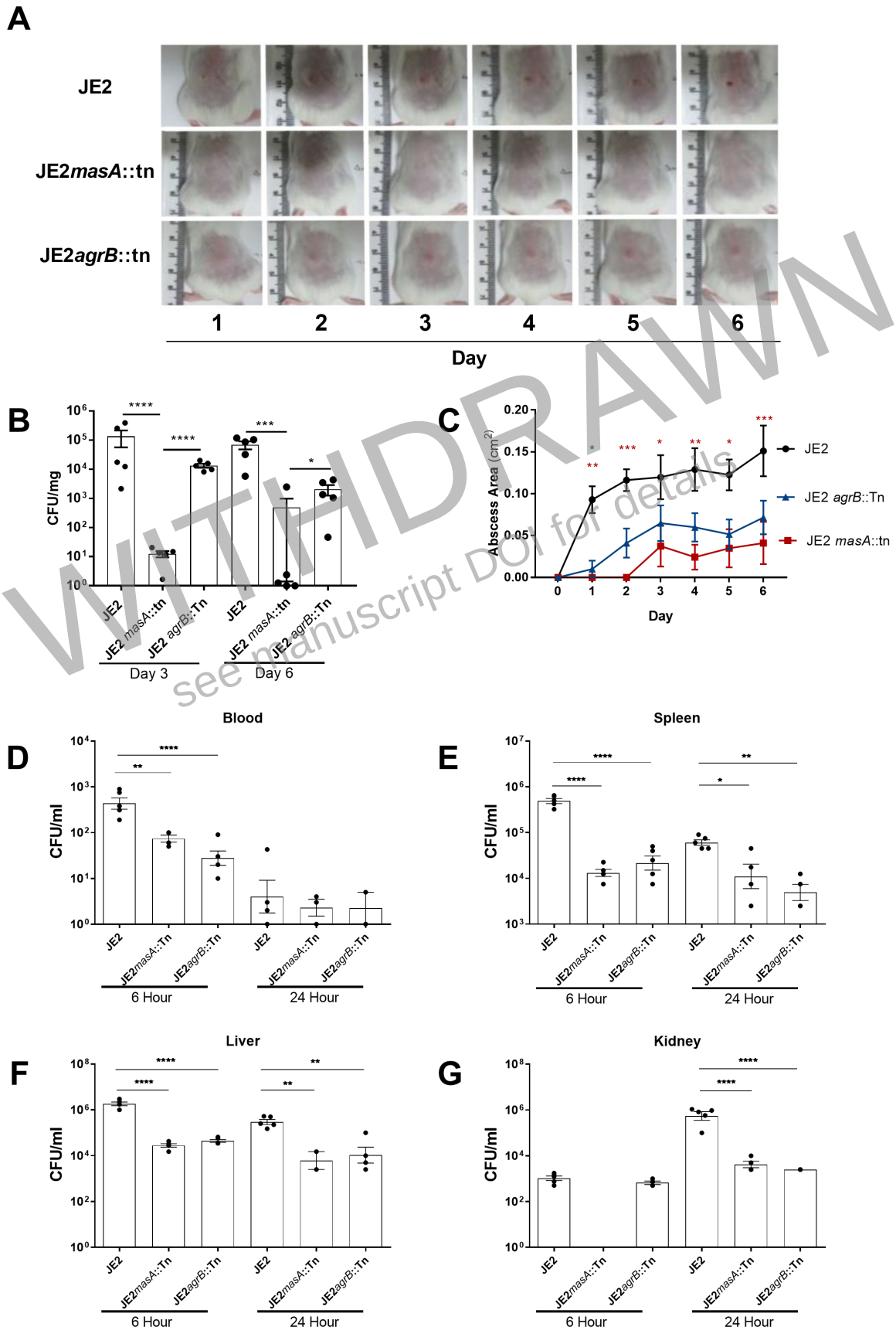

Figure 3

The inactivation of *masA* affects the ability of *S. aureus* to cause disease in both a superficial and systemic infection model. Balb/c mice were infected subcutaneously with $2x10^7$ CFU wild type (JE2), and isogenic strains in which the *masA* and *agrB* genes were inactivated. (**a**) Abscess lesion area was assessed daily and representative lesions from the dorsal area of mice from each group are shown, and results are expressed as total lesion size (cm^2) ± SEM (**b**). The bacterial burden in the skin was assessed by viable counting at 3 and 6 days post-infection (**c**). (**d-g**) C57 mice were inoculated via tail vein injection of $2x10^7$ CFU the wild type JE2 *S. aureus* strain and the *masA* and *agrB* mutants. (**d-g**) The tail vein of mice were inoculated with a sub-lethal dose of the wild type JE2 *S.* Blood (**d**), spleens (**e**), livers (**f**) and kidneys (**g**) were harvested at 6 and 24hours post infection and the burden of bacteria in each sample was quantified. For the superficial infection, n=10 representative of 2 independent pooled experiments. For the systemic infection, n=5 of one independent experiment. Statistics were performed using One Way Anova with a Turkey post-test (superficial) and Sidak's multiple comparison test (systemic) and significance was determined as < *0.05; **0.01; ***0.001; ****0.0001.

Iron homeostasis is affected in the absence of MasA.

Given the relatively small size of the MasA protein (105 residues), and that the majority of it (73%) is predicted to be embedded in the bacterial membrane, we sought to determine how its loss can have such a detrimental effect on the pathogenicity of *S. aureus*. We adopted a proteomic approach and used tandem mass tagging coupled to mass spectroscopy (TMT-MS[22]) on whole cell lysates of the JE2 strain and its *masA* mutant. Using the *S. aureus* NCTC 8325 proteome as our reference we were able to detect and quantify the abundance of 1149 proteins. Using a 2-fold difference in abundance as our cut-off for biological significance we found 63 proteins differentially abundant in the *masA* mutant compared to the wild type strain (Supplementary Table 1). Of these differentially abundant proteins, of note was that many proteins involved in both the uptake (e.g. IsdB and IsdC[23]) and efflux (HrtA and HrtB[24]) of heme-iron were affected (Table 1), suggesting that the ability of the bacteria to control iron homeostasis may be impaired in the *masA* mutant. To explore this further we compared the levels of intracellular iron in the wild type and mutant strains using the antibiotic streptonigrin which causes nucleic acid damage in the presence of iron[25], and as such quantifying the level of sensitivity of a bacterium to this antibiotic can be used as an indication of the relative amounts of iron present in the bacterial cytoplasm. In both the JE2 and SH1000 backgrounds the *masA* mutants had higher levels of intracellular iron, indicated by increased sensitivity to streptonigrin when compared to their wild type strains (Fig. 4A and B).

S. aureus, like many other pathogens, utilizes heme as a source of iron during infection[26]. It can either capture hemoglobin and release heme from this, or synthesise it endogenously using the enzymes encoded by the *hem* locus[27]. In the *masA* mutant, while the increased abundance of the Isd heme uptake system proteins might explain the observed increased levels of intracellular iron, this system is specific to heme, and TSB, the medium used to grow the bacteria contains negligible amounts of this. The Hrt efflux system is also highly specific for heme, and that we see an increased expression of this suggest that it is responding to increasing levels of heme-iron within the bacterial cells. However, as its function is to pump heme out of the cells, that we see increased iron level despite increased expression of this efflux system suggest that its activity may be impaired. Interference in the stoichiometry of ATPases and their permeases has been shown previously to significantly affect the activity of *S. aureus* efflux systems[28]. In the MasA mutant we see an almost 18-fold increase abundance of the HrtB protein (the permease) but only a 2.7-fold increase abundance of the HrtA protein (the ATPase), which is intriguing, given that these genes are co-transcribed. It is therefore possible that the observed differences in relative abundance of the Hrt proteins may be affecting its efflux activity, which would consequently affect the ability of the bacteria to reduce their intracellular heme levels.

To examine whether the activity of the Hrt system was impaired in the *masA* mutant, despite the HrtA and HrtB proteins being more abundant, we developed an heme adaptation assay. The bacteria were grown overnight in either TSB or TSB supplemented with hemin, and these bacteria were then used to inoculate fresh TSB with increasing concentrations of hemin where the ability of the bacteria to adapt to this was determined by quantifying their density after 8 hours of growth (Fig. 4C). Pre-exposure of the bacteria to hemin (in the overnight cultures) enabled the wild type bacteria to adapt to the increasing concentrations of hemin as illustrated by the higher density of the bacterial cultures after 8 hours of growth (Fig. 4D and E). However, in both backgrounds, the *masA* mutants were impaired in their ability to adapt to the presence of hemin. This suggests that despite the increased abundance of the Hrt proteins, the efflux

activity of this system is impaired, which provides an explanation for the increased intracellular iron concentrations observed above (Fig 4A and B).

Table 1 Differentially regulated iron process proteins in the absence of MasA

Accession[#]	Protein Function Description	Fold Change[€]	*p*-Value*
Q2FVR0	Hemin transport system permease protein HrtB	17.97 ↑	< 0.0001
Q2FVR1	Hemin import ATP-binding protein HrtA	2.7 ↑	0.005
Q8KQR1	Iron-regulated surface determinant protein C	2.56 ↑	0.001
Q2FWZ8	Bacterial non-heme ferritin	2.11 ↓	0.0005
Q2FZF0	Iron-regulated surface determinant protein B	2.08 ↑	0.079
Q2G1Z3	Iron compound ABC transporter	2.06 ↑	0.002

[#]Accession corresponds to protein identifier in UniProt database.
[€]Fold change in the abundance of proteins in the masA mutant relative to the wild type strain in three independent experiments.
**p*-Value was calculated using the Student's *t*-test

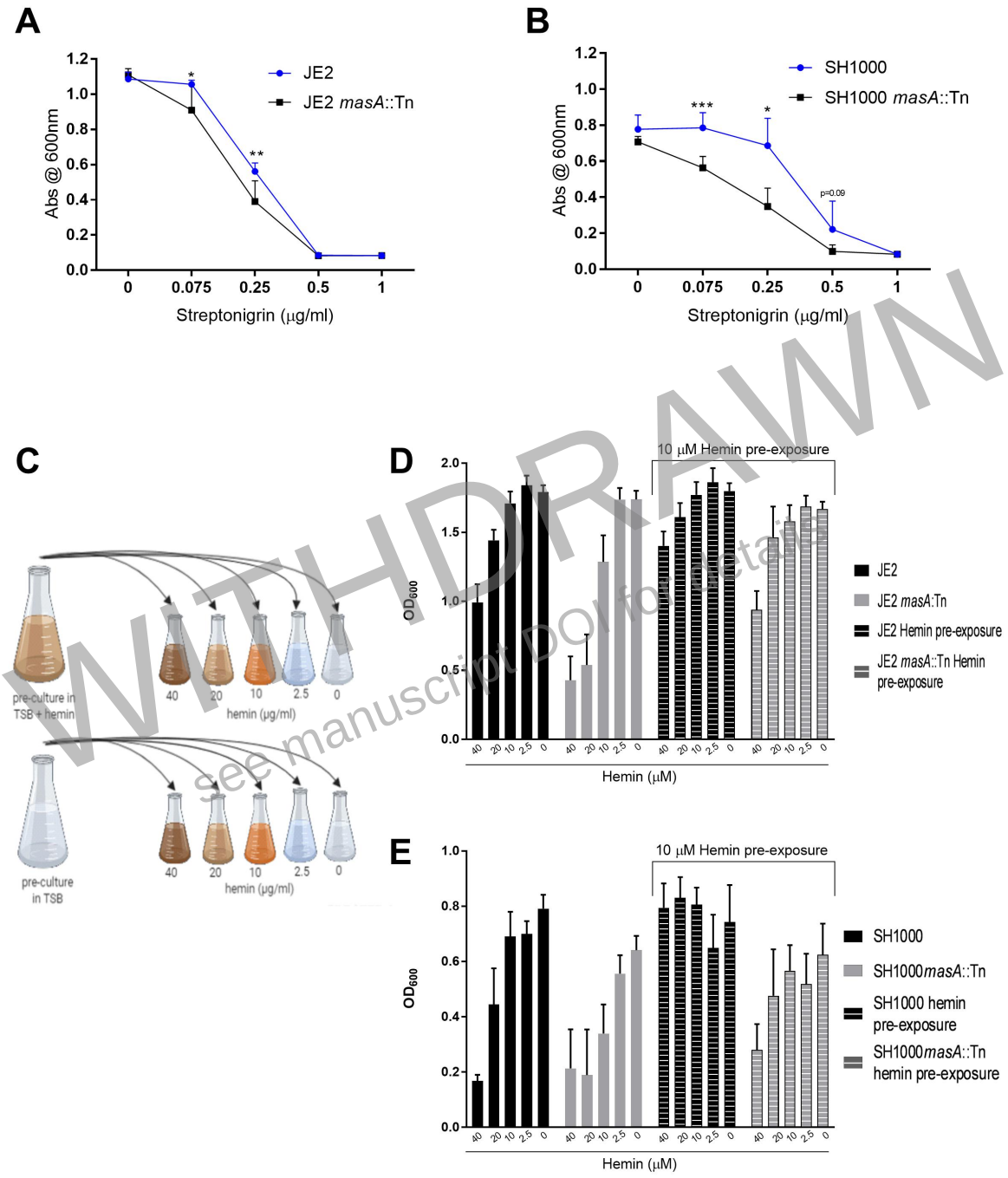

Figure 4

(a) Growth of both JE2 and SH1000 in the presence of streptonigrin was determined at 8 hours at various streptonigrin concentrations (**A** and **B**). Streptonigrin was consistently more effective at inhibiting the growth of *masA* deficient strains, indicating they have higher levels of intracellular iron. (**C**) To determine the role of *masA* in bacterial adaptation to hemin-rich environments, bacteria were cultured either in normal TSB, or TSB supplemented with moderate hemin. Bacteria were then sub-cultured into a range of hemin concentrations. Pre-culture in moderate hemin conferred an advantage for subsequent growth in high hemin concentrations in both JE2 and SH1000 backgrounds (striped bars **D** and **E**). The loss of *masA* was disadvantageous for adaption to high hemin environments (grey bars **D** and **E**). Statistics

were performed using the Student's paired *t*-test and significance was determined as < *0.05; **0.01; ***0.001.

Increased intracellular iron concentrations affects the toxicity and immune evasion capabilities of *S. aureus*.

Previous work on the Hrt system demonstrated that increased intracellular iron can affect protein secretion[29]. As such, we sought to determine whether the increased levels of iron that result from the loss of MasA could explain the loss of the toxicity and immune evasion capabilities of the mutants. To address this, we grew the wild type JE2 and SH1000 strains in TSB with increasing concentrations of hemin, where 10 µM was the highest concentration we could use that did not affect the rates of bacterial growth upon first exposure. Using streptonigrin we demonstrated that although the bacteria can adapt to this, the higher the level of hemin in their growth media, the higher the level of heme-iron in their cytoplasm (Supplementary Fig. 3A and B). As this was comparable to the iron level we observed in the *masA* mutant, we harvested the bacterial supernatant and demonstrated that this resulted in a decrease in cytolytic activity as measure by THP-1 lysis in both backgrounds (Fig. 5A and B). Increasing levels of hemin resulted in decreased secretion of the PSM family of toxins (Supplementary Figure 3C and D). We also verified that as with the *masA* mutant, the effect the increased iron had on toxicity was mediated through the repression or lack of activation of the Agr quorum sensing system (Fig. 5C and D). Increased levels of intracellular iron also affected the level of staphyloxanthin produced by the bacteria (Fig. 5E and F). Together these data suggest that the effect the loss of MasA has on iron homeostasis is contributing to the effect we have observed in its offensive and defensive capabilities. There are however other as yet uncharacterised features involved here. We examined the toxicity of HrtA and HrtB mutants (which has altered intracellular heme levels) as well as a Fur (the ferric uptake regulator that is also required for heme homeostasis[30]) mutant in the JE2 background. While we observed a small drop in toxicity of the HrtB mutant, there was no difference between the HrtA or Fur mutants when compared to the wild type strain (Supplementary Figure 4), suggesting that as yet unidentified factors in addition to heme accumulation must be

361 contributing to the effects observed when MasA is inactivated. Further molecular
362 characterisation of the activity of MasA is currently underway.

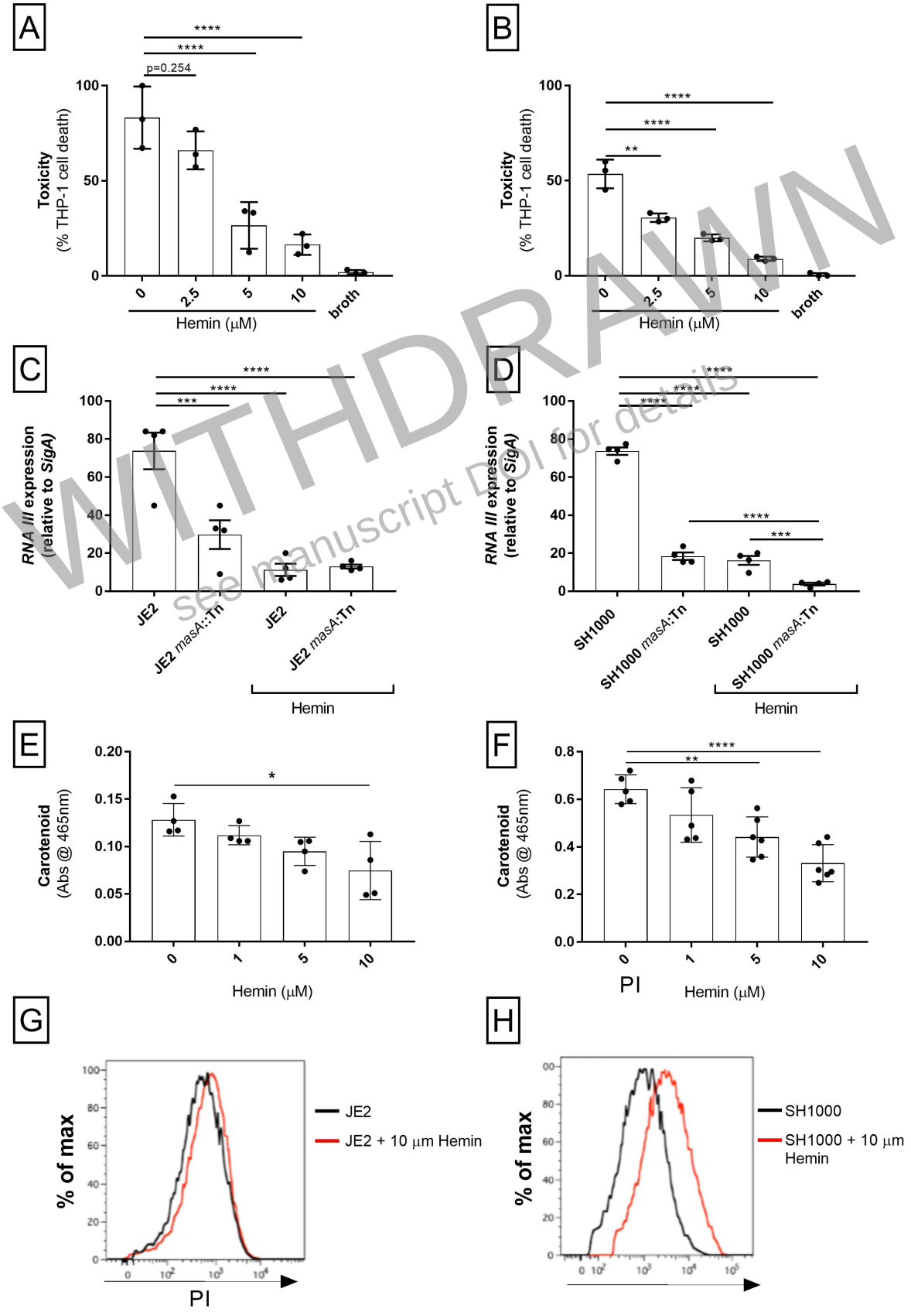

363

Figure 5

When cultured in increasing concentrations of hemin, the ability of JE2 (**A**) and SH1000 (**B**) to cause toxicity in THP-1 cells is diminished in a concentration dependent manner. (C) Transcript levels of *rnaIII* are, compared to levels of *masA* deficient JE2 and SH1000, further diminished in both backgrounds when exposed to hemin (**C** and **D**). Carotenoid biosynthesis is also diminished during culture in additional hemin, and this effect was observed in a concentration dependent manner in both backgrounds (**E** and **F**). (**G** and **H**) Representative images of FACS analysis are shown. A shift in the PI signal for JE2 and SH1000 supplemented with hemin and stained with PI demonstrates a decrease in membrane integrity. Statistics were performed using the Student's paired *t*-test and significance was determined as < *0.05; **0.01; ***0.001.

Discussion

As a major global cause of morbidity and mortality, many diverse strategies have been developed and tested to control and treat *S. aureus* infections. Vaccination, for example has been successfully used to control and reduce the incidence of many bacterial infections. However, despite significant investment and multiple diverse *S. aureus* components including toxins, surface expressed proteins and capsule being targeted, vaccines have provided no significant level protection when used in human trials[31]. Recent studies on populations of clinical isolates may provide an answer to some of these failures, where significant variability in the expression of toxins and capsule has been demonstrated[12-14,32]. The isolates not expressing the target would therefore evade the immune response elicited by the vaccine, affecting its coverage and effectivity. This population level variability in the expression of these virulence factors has only recently been demonstrated, and it's unlikely that these *S. aureus* components would have been considered good vaccine targets, were this information available at the time. So, it would appear that our lack of understanding of the complexity of the pathogenicity of *S. aureus* is hampering the development of an effective vaccine.

The *S. aureus* research field has benefitted greatly from the development of next generation sequencing technologies, with thousands of isolates having been sequenced to date. Given

the proportion of uncharacterised coding regions on the *S. aureus* genome is it perhaps unsurprising that we do not yet fully understand its pathogenicity. With many genes described only as encoding hypothetical proteins, or ascribed a putative function based on amino acid homology to other characterised proteins, it is clear we have much to learn about this microbial pathogen. In recent work we have developed a functional genomics approach to begin to bring genome sequence data and the study of *S. aureus* pathogenicity together[12-14,28]. In doing so we have identified several novel effectors of the ability of *S. aureus* isolates to secrete cytolytic toxins, one of which is MasA, a putative membrane bound protein. In two distinct *S. aureus* backgrounds we demonstrate the role this protein plays in both the ability of this pathogen to secrete cytolytic toxins and protect itself from several aspects of the innate immune system.

Although the precise activity of this protein has yet to be elucidated, we have summarised in figure 6 what we understand to date. The effect it has on the activity of the Hrt heme efflux system is such that intracellular levels of heme iron are elevated, and this contributes to some of the pathogenicity related phenotypes we have observed for the *masA* mutant. It is possible that given its likely membrane localisation that the MasA protein may be directly interacting and enhancing the activity of the Hrt proteins. However, were this the case we would expect to see the same effect on toxicity when we inactivate the Hrt system by mutagenesis, which we don't (Supplementary Fig. 4), suggesting additional or alternative activities for MasA. So although we can phenocopy the loss of MasA (with respect to toxicity and staphyloxanthin production) by increasing intracellular iron levels through the addition of hemin to the bacterial growth media, we don't see the same effect when we increase intracellular iron levels through the inactivation of the Hrt system.

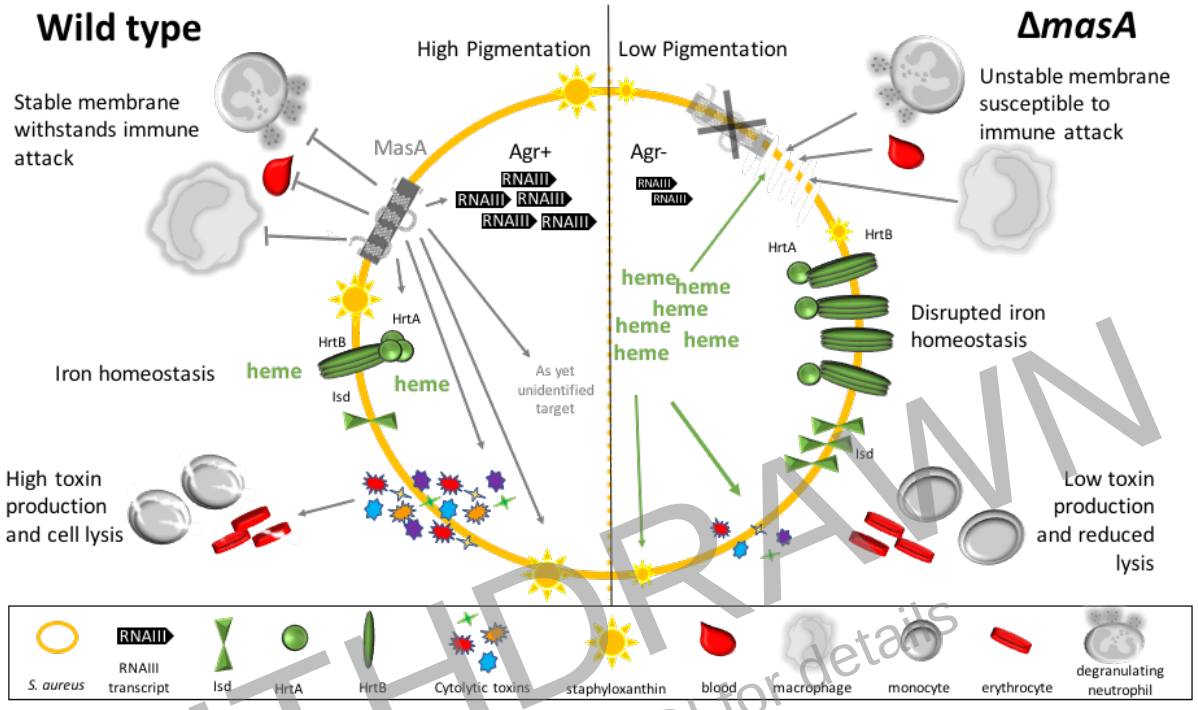

Figure 6
Summary of the effect the inactivation of the *masA* gene has on the bacterial cell. In the absence of MasA the bacteria are unable to protects itself from membrane attack and phagocytosis. The Agr system is does not become activated, which subsequently affects the production of cytolytic toxins. The abundance and stoichiometry of the Hrt proteins is also affected in the *masA* mutant, which affects heme-iron homeostasis, and this partially contributes to the toxic and immune susceptibility phenotypes reported here.

Our current hypothesis is that with such a large proportion of the protein predicted to be embedded in the bacterial membrane, and that the gross phenotypic changes to its toxic and immune evasion capabilities are mediated by other diverse membrane bound molecules (i.e. AgrB, AgrC, staphyloxanthin and HrtB) that it may have a more general role in stabilising the bacterial membrane so that all of these diverse proteins can perform optimally. In support of this more generalist activity, we found homologues of MasA in all staphylococcal species, but also in other diverse bacterial genera including *Streptococcus pneumoniae* and the Gram negative *Vibrio cholerae.* An alignment of these MasA homologues indicates a high level of conservation suggesting it evolved before these bacteria diverged (fig. 7). While *Streptococcus pneumoniae* has a HrtB protein, *Vibrio cholera* doesn't, suggesting that the role of MasA is not limited to interacting with this heme efflux system. Future work to elucidate the molecular details of the activity of MasA is currently underway, and given the widespread

prevalence of this protein, this work is likely to have widespread implications to our understanding of the biology of many diverse bacteria.

```
S. pseudo.      ----------------------MYLVVAYISIFKMRIMMPKLLRVIMGLLLIIVVATSLVYYPASTWWVFVVLILLIGNVEITAFKHSKNDEKGVRILNMMSLFILVIYIVLVAVFI 95
Strep. pneumo.  -----------------------------------VVFTRILRIIMGVLLLFVLALTTMSFPKENWWVFIVLLLLVGNVEVTGFKMLKKDLKGVNILNLMSLFIFVIYFILTIVLF 81
S. aureus       -----------MQFYLILLAILYLIVSFISIFKMEVVFTRILRIIMGVLLLFVLALTTMSFPKENWWVFIVLLLLVGNVEVTGFKMLKKDLKGVNILNLMSLFIFVIYFILTIVLF 105
Vibrio cholerae ----------------------------------MEVVFTRILRIIMGVLLLFVLALTTMSFPKENWWVFIVLLLLVGNVEVTGFKMLKKDLKGVNILNLMSLFIFVIYFILTIV- 81
S. argenteus    -----------MQFYLILLAILYLIVSFISIFKMEVVFTRILRIIMGVLLLFVLALTTMSFPKENWWVFIVLLLLVGNVEVTGFKMLKKDLKGVNILNLMSLFIFVIYFILTIVLF 105
S. pettenkoferi -----------MQLYLILLPILYLIVAYISIFKMKTIFTTILRIIMALLLLFVVALTTVSFPAANWWVFVVLFLLVANVEITGFKHSKHDKKGVRLLNILTVILFVIYLILTIVMY 105
S. cohnii       -----------MQLYLIFLPVLYLIVSYXSIFKMNTIITRILRIIMSLLLLFVVAITTLSFPAINWWVFIVLLLIIGNVEITAFKNSKNDQKAVQILNIMSVILFVIYVILTLVLY 105
S. lugdunensis  MIGSGLERKSKMQLYLILLPILYLIVSYISIYKMPTIFTRILRIIMGILLLFVIAITTLQFPTENWWVFIVLLLLVGNVEVTGFKAIKQDRKGLLILNLLTLLLYIVYLILVFIMY 116
S. warneri      -----------MKLYLILLPLLYLIVSYISIFKMNSIFTRILRIIMAVLLLFVVAITTMQFPNENWWVFIVLLLLVGNVEVTAFKSLKNDVKGVNILNILSIGLF---------- 94
S. haemolyticus -----------MKLYLLLLPVLYLIVSYISIFKMHSIFIRILRIIMGVLLLFVLALTTLQFPAENWWVFVVLALLVGNVEVTAFKALKHDAKAVSILNILSVILFVIYIILIFVMY 105
                                                ::  :**:**.:**::*:* : : :*  .****:** *::.***:*.**  *:* *.: :*::::: :
```

Figure 7
Alignment of the amino acid sequence of MasA homologues in other staphylococcal species, and other bacterial genera. The length of the predicted proteins are indicated on the right. The * indicates positions which have a single, fully conserved residue, while : indicates conservation between residues with strongly similar properties.

While the study of small numbers of 'lab strains' has enabled us to gain a level of understanding of *S. aureus* pathogenicity, we believe our work demonstrates the potential for vastly increasing our understanding by adopting a population level approach. Perhaps the biggest problem with tackling this pathogen is that the vast majority of its interactions with humans is as a commensal organism, so it is well adapted to exposure to the aspect of our immune system present in our nasal mucosa. As such, a single protein that affects both virulence and immune evasion, and is present across diverse genera of pathogenic bacteria represents a promising target for future broad-spectrum therapeutic intervention strategies.

Acknowledgements

This work was funded by a BBSRC Grant awarded to RCM, an Intramural Research Program (NIAD, NIH) awarded to MO, a PhD studentship funded by the Saudi Arabian Government awarded to AA, and both RCM and RMM are Wellcome Trust funded Investigators. Thanks also go to Borko Amulic and Fernando M. Ponce-Garcia for providing the human erythrocytes, and Alanna Kelly and Jenny Mannion for assistance with mice culling.

Materials and Methods

Ethics Statement

Peripheral blood from healthy donors was acquired in accordance with the Declaration of Helsinki and approved by Research Ethics Committee (REC 18/EE/0265). All animal experiments were conducted in accordance with the recommendations and guidelines of the health product regulatory authority (HPRA), the competent authority in Ireland and in accordance with protocols approved by Trinity College Dublin Animal Research Ethics Committee.

Bacterial strains and growth conditions

A list of *S. aureus* strains used in this study can be found in Table 1. *S. aureus* strains were routinely grown in Tryptic Soy broth (TSB), or Brain Heart Infusion (BHI) where indicated. Overnight cultures were used to inoculate fresh media at a dilution of 1:1,000 and then grown for 18 h at 37 °C in air with shaking (180 rpm). For transposon mutants, erythromycin (5 µg/mL) was added to the growth medium. For complementation with pRMC2 plasmid (14) containing the *masA* gene (p*masA*), anhydrous tetracycline (50-200 ng/mL) was included in the growth medium. The toxin-containing supernatant for each bacterial strain was harvested by centrifugation at 10,000 x *g* for 10 min. Hemin (CAS 16009-13-5) and Streptonigrin (CAS 3930-19-6) were included in culture media at the indicated concentrations.

Table 2: Bacterial strains used in this study.

Strain	Description	Reference
JE2	USA300; CA-MRSA, type IV SCC*mec*; lacking plasmids p01 and p03; wild-type strain of the NTML	16
JE2*agrB*::Tn	Accessory gene regulator B (*agrB*) transposon mutant in JE2	16
JE2*masA*::Tn	*masA* transposon mutant in JE2	16
JE2*masA*::Tn p*masA*	*masA* transposon mutant complemented with *masA* gene housed in pRMC2 expression plasmid	This study
SH1000	Laboratory strain, 8325-4 with a repaired *rsbU* gene; SigB positive	14
SH1000*masA*::Tn	*masA* transposon mutant in SH1000	This study
SH1000*masA*::Tn p*masA*	*masA* transposon mutant complemented with *masA* gene housed in pRMC2 expression plasmid	This study
JE2*sigB*::Tn	Sigma B transposon (*sigB*) mutant in JE2	16

Genetic manipulations involving *masA*

The *masA* gene was amplified by PCR from JE2 using Phusion high-fidelity DNA polymerase (NEB) and primers MasFW: CG**GGTACC**GAACCCTTTGAAACG (KpnI; Tm 64.2 °C) and MasRV: GC**GAGCTC**GTTGCAATTATGTTATTGC (SacI; Tm 63.4 °C) and cloned into the tetracycline inducible plasmid pRMC2 to make p*masA*. This was electroporated into S. aureus RN4220 and subsequently into JE2 to complement the *masA* transposon mutant. DNA from JE2*masA*::Tn was transduced into wild-type SH1000 by transduction with ϕ11 as described previously (23) and transductants containing the inserted transposon were screened on TSA containing erythromycin (10 µg/mL). SH1000*masA*::Tn was verified for Tn insertion of *masA* by colony PCR using the above *masA* primers.

Monocyte (THP-1) toxicity

The monocytic THP-1 cell line (ATCC TIB-202) was used as previously described (8). Briefly, cells were grown in 30 mL of RPMI-1640, supplemented with heat-inactivated fetal bovine serum (10 %), L-glutamine (1 µM), penicillin (200 units/mL) and streptomycin (0.1 mg/mL) (defined as complete medium) in a humidified incubator at 37°C with 5% CO_2. For toxicity assays, cells were harvested by centrifugation at 400 x *g* and resuspended to a final density of 1-1.5 x 10^6 cells/mL in tissue-grade phosphate buffered saline (PBS), typically yielding > 95% viability assessed by trypan blue exclusion and easyCyte flow cytometry.

Bronchial epithelial cell (A549) toxicity

A549 cells were grown in complete media. When confluent (80-90%), cells were detached with trypsin EDTA (0.25% ThermoFisher), resuspended, centrifuged for 10 min at 400 x *g* and resuspendend to 1-1.5 x 10^6 cells/mL in tissue grade PBS. To determine *S. aureus* toxicity 75 µL of bacterial supernatant (Neat, 75%, 50% and 25%) were incubated with 75 µL of A549 cells in 96 well plate for 20 min at 37 °C. Cell lysis was measured as lactate dehydrogenase release using the CytoTox 96 Non-Radioactive Cytotoxicity Assay (Promega) according to manufacturer's instructions. Experiments were done in triplicate three times and results represent the mean ± SD.

Human red blood corpuscle Toxicity

Human red blood corpuscles (RBCs) were isolated from heparinized venous blood obtained from healthy adult volunteers. RBCs were washed twice in sterile saline (0.9% NaCl) and centrifuged at 600 x *g* for 10 min. RBCs were diluted to 1% in PBS and 200 µL was incubated with 50 µL of bacterial supernatant in a 96 well plate for 30 min at 37 °C. Plates were centrifuged for 5 min at 400 x *g* supernatants transferred to a sterile 96 well plate and RBC

lysis evaluated by determining the absorbance at 404_{nm}. Saline and 0.5% Triton X-100 were used as negative and positive controls respectively.

Toxin expression quantification

For alpha toxin overnight cultures of *S. aureus* were diluted 1:1,000 in 5 mL TSB and incubated for 18 h at 37°C with shaking (180 rpm). Bacteria were normalized to an OD_{600} of 2, centrifuged for 10 min at 10,000 x *g*, supernatant removed and proteins precipitated using trichloroacetic acid (TCA) at a final concentration of 20% for 2 h on ice. Samples were centrifuged at 18,000 x *g* for 20 min at 4°C, washed three times in ice-cold acetone and solubilized in 100 µl 8 M urea. Proteins (10 µl of each sample) were mixed with 2x-concentrated sample buffer and heated at 95°C for 5 min before being subjected to 12% SDS-PAGE. Separated proteins were wet transferred onto a nitrocellulose membrane and afterwards blocked overnight in 5% semi-skimmed milk at 4°C. Membranes were washed and incubated with polyclonal antibodies specific for alpha-toxin (1:5,000 dilution; Sigma-Aldrich) for 2 h at room temperature. Membranes were washed and incubated with horseradish peroxidase-coupled protein G (1:1,000; Invitrogen) for 1 h at room temperature. Proteins were detected by using the Opti-4CN detection kit (Bio-Rad). The Western blots were performed in triplicate, and the bands were scanned and quantified by using ImageJ software (http://rsbweb.nih.gov/ij/). For Phenol soluble modulin (PSM) quantification, including delta toxin were measured using reverse-phase high performance liquid chromatography/mass spectrometry (RP-HPLC/MS) as described previously (24).

qRT-PCR

Cultures of *S. aureus* grown overnight in TSB were diluted 1:1,000 in fresh TSB and grown at 37°C for 7 h. Cultures were normalised based on OD_{600} measurements prior to RNA isolation. Cultures were treated with two volumes of RNAprotect (Qiagen) incubated for 10 min at room temperature, centrifuged and the pellet was resuspended in Tris-EDTA (TE) buffer (Ambion) with lysostaphin (5 mg/mL) and incubated for 1 h, followed by proteinase K treatment for 30 min. RNA was isolated using the Quick-RNA kit (ZYMO RESEARCH). RNA was quantified using a NanoDrop (Thermo Fisher Scientific). Reverse transcription was performed using the qScript cDNA Synthesis Kit QuantaBio) according to manufacturer's instructions using random primers. Standard curves were generated for both *sigA* [29] (Forward: 5'-AACTGAATCCAAGTCATCTTAGTC- 3' and reverse: 5'-TCATCACCTTGTTCAATACGTTTG-3') and *rnaIII* (Forward: 5'-GAAGGAGTGATTTCAATGGCACAAG- 3' and reverse: 5'-TCATCACCTTGTTCAATACGTTTG- 3') primers using genomic DNA to determine efficiency. Real-time PCR was performed using the SYBR Green QPCR Mix (NeoBiotech) and the Mic qPCR Cycler (bio molecular systems). Cycling conditions were 95°C for 10 min followed by

40 cycles of 95°C for 15 s and 60°C for 1 min and a dissociation step 95°C for 15 s and 60°C for 1 min. Cycle threshold values were determined for at least 3 biological repeats. For each reaction, the ratio of RNA III and *gyrB* transcript number was calculated as follows: 2(Ct gyrB – Ct RNAIII).

Carotenoid pigment analysis

Carotenoid pigment analysis was performed as described previously [19] with minor modifications. Overnight bacterial cultures were used to inoculate 5 mL of fresh TSB in a 1:1,000 dilution which was subsequently grown for 24h at 37°C with shaking (180 rpm). 1 ml of bacterial culture was centrifuged for 10,000 x *g* for 5 min, supernatant discarded, and cells resuspended in 500 µl 100% methanol. Cells were heated for 3 min at 55°C in a water bath, vortexed and centrifuged at 10,000 x g for 2 min to remove cell debris and extraction repeated twice. The absorbance of the methanol extracts was measured at 465_{nm} using a photometer (SPECTROstar Nano, BMG Labtech). JE2*sigB*::Tn was used a negative control.

SDS-Stability

The *S. aureus* strains were grown overnight in TSB, used at a 1:1000 dilution to inoculate TSB containing a range of concentrations of sodium dodecyl sulphate (sigma). The ability of the withstand the membrane damaging effect of the detergents was determined by quantifying bacterial growth (OD_{600}) after 24 hours.

Membrane-Stability

The *S. aureus* strains were grown overnight in TSB, or TSB containing varying concentrations of hemin. Cells were harvested by centrifugation, resuspended in PBS to a concentration of 1 x 10^6 cells per ml. 100 µl of bacterial cells were incubated with PI for 5 minutes at room temperature prior to flow cytometric analysis on a Novocyte (ACEA Biosciences). Data were analysed using FlowJo 10.5

Oleic acid susceptibility

Bacteria were grown overnight, subcultured 1:1,000 in fresh TSB and grown for 18h. Bacteria were washed twice in 2M NaCl-2mM EDTA buffer, normalised to an OD_{600} of 1, and further diluted 1:1,000 in above buffer. Oleic acid (Sigma) was initially dissolved in ethanol and working solution were further prepared in 2M NaCl-2mM EDTA buffer. 100 µl of cells were incubated with either 100 µl of buffer or oleic acid solution (6 µg/mL final concentration) in duplicate for 1 h at 37°C. Bacteria were enumerated following dilution in PBS and plating onto TSA. Bacterial survival was calculated by dividing the number of bacteria from wells containing oleic acid by bacteria from wells containing control.

608

609 **Antimicrobial peptide susceptibility**

610 Human neutrophil defensin-1 (hNP-1) (AnaSpec Incorporated, California, USA) susceptibility
611 assay was performed as described previously (15). Briefly, a final inoculum of 10^5 CFU was
612 resuspended in 1 % BHI supplemented with 10 mM potassium phosphate buffer and a final
613 concentration of 5 µg/mL of hNP-1 and incubated for 2 h at 37 °C. Final bacterial concentration
614 was evaluated by serial plating onto TSA plates and data represented as mean (± SD) percent
615 survival CFU.

616

617 **Phagocytosis assay**

618 THP-1 cells (tested were harvested by centrifugation and resuspended in fresh complete
619 medium to 2 x 10^5 cells/mL. Monocytes were differentiated by the addition of phorbol 12-
620 myristate 13-acetate (PMA) at a final concentration of 100 nM and 500 µL of cells were added
621 to a tissue culture treated 24 well plate (Nunc) for 48 h. THP-1 cells were washed twice in
622 tissue grade PBS and incubated with complete medium 24 h before infection. Two hours
623 before infection, THP-1 cells were washed twice in PBS and cells incubated in complete media
624 without antibiotics. Bacterial strains were grown overnight, diluted 1:100 in fresh TSB and
625 grown to an OD of 0.3. Bacterial cells were washed twice in PBS and an MOI of 1 was
626 established to infect THP-1 cells. Plates were centrifuged at 300 x *g* for 5 min to synchronise
627 phagocytosis and incubated at 37°C with 5% CO_2 for 1 h. Following 1 h incubation, media was
628 discarded, cells washed four times in PBS and wells incubated with RPMI media containing
629 gentamicin (200 µg/mL) and lystostaphin (20 µg/mL) for 1 h. Media was discarded and wells
630 for 2 h time points were lysed with triton X-100 (0.01%) and CFU enumerated on Tryptic soy
631 agar (TSA) plates and wells for 6 h analysis were further incubated in RPMI containing no
632 antibiotics and processed as above.

633

634 **Streptonigrin Susceptibility Assay**

635 Normalised OD_{600} overnight cultures were diluted 1:100 in PBS and 100 µl were mixed with 3
636 ml 0.5% agar and poured over TSA plates. When dry, 1.5 µl of streptonigrin (2.5 mg/ml;
637 dissolved in DMSO) was spotted onto the plate. Plates were incubated at 37°C for 18 hours
638 and zones of clearance were measured. Data are represented as area of the growth inhibition
639 zone.

640

641 **Mice**

642 Age (6-8 weeks) and sex matched wild-type BALB/c mice were purchased from Charles River
643 Laboratories UK. Mice were housed under specific pathogen-free conditions at the Trinity
644 College Dublin Comparative Medicines unit. All animal experiments were conducted in

accordance with the recommendations and guidelines of the health product regulatory authority (HPRA), the competent authority in Ireland and in accordance with protocols approved by Trinity College Dublin Animal Research Ethics Committee.

Murine subcutaneous abscess model

The dorsal backs of mice were shaved and injected subcutaneously with *S. aureus* (2 x 10^7 CFU) in 100 µl of sterile PBS using a 27-guage syringe (BD Biosciences). Measurements of abscess lesion area (cm^2) were made by analysing digital photographs using M3 Vision software (Biospace Lab) and pictures contain a millimetre ruler as a reference. To determine the bacterial burden, 8mm punch biopsies of lesional skin were taken at day 3 and 6 post-infection. Tissue was homogenized in sterile PBS and total bacterial burden was determined by plating out serial dilutions on TSA.

Murine bloodstream infection model

5X10^7 cells of JE2, JE2masA::tn or JE2agrB::tn via tail vein injection. Mice culled at 6 and 24 hours. Blood was collected by cardiac puncture. Liver, spleen and kidney were harvested and homogenised in 1ml of PBS. Bacterial burdens were established by plating out serial dilutions of blood and organ homogenates on TSA.

Protein extraction, TMT labelling and high pH reversed-phase chromatography

Aliquots of 100 µg of up to ten samples per experiment were digested with trypsin (2.5 µg trypsin per 100 µg protein; 37 °C, overnight), labelled with Tandem Mass Tag (TMT) ten plex reagents according to the manufacturer's protocol (Thermo Fisher Scientific) and the labelled samples pooled. An aliquot of the pooled sample was evaporated to dryness and resuspended in buffer A (20 mM ammonium hydroxide, pH 10) prior to fractionation by high pH reversed-phase chromatography using an Ultimate 3000 liquid chromatography system (Thermo Fisher Scientific). In brief, the sample was loaded onto an XBridge BEH C18 column (130 Å, 3.5 µm, 2.1 mm × 150 mm, Waters, UK) in buffer A and peptides eluted with an increasing gradient of buffer B (20 mM ammonium hydroxide in acetonitrile, pH 10) from 0 to 95% over 60 min. The resulting fractions were evaporated to dryness and resuspended in 1% formic acid prior to analysis by nano-LC MSMS using an Orbitrap Fusion Tribrid mass spectrometer (Thermo Scientific).

Nano-LC mass spectrometry

High pH RP fractions were further fractionated using an Ultimate 3000 nanoHPLC system in line with an Orbitrap Fusion Tribrid mass spectrometer (Thermo Scientific). In brief, peptides in 1% (vol/vol) formic acid were injected onto an Acclaim PepMap C18 nano-trap column

(Thermo Scientific). After washing with 0.5% (vol/vol) acetonitrile 0.1% (vol/vol), formic acid peptides were resolved on a 250 mm × 75 μm Acclaim PepMap C18 reverse phase analytical column (Thermo Scientific) over a 150 min organic gradient, using seven gradient segments (1–6% solvent B over 1 min, 6–15% B over 58 min, 15–32% B over 58 min, 32–40% B over 5 min, 40–90% B over 1 min, held at 90% B for 6 min and then reduced to 1% B over 1 min) with a flow rate of 300 nl min^{-1}. Solvent A was 0.1% formic acid and solvent B was aqueous 80% acetonitrile in 0.1% formic acid. Peptides were ionised by nano-electrospray ionisation at 2.0 kV using a stainless steel emitter with an internal diameter of 30 μm (Thermo Scientific) and a capillary temperature of 275 °C.

All spectra were acquired using an Orbitrap Fusion Tribrid mass spectrometer controlled by Xcalibur 2.0 software (Thermo Scientific) and operated in data-dependent acquisition mode using an SPS-MS3 workflow. FTMS1 spectra were collected at a resolution of 120,000 with an automatic gain control (AGC) target of 200,000 and a max injection time of 50 ms. Precursors were filtered with an intensity threshold of 5000 according to charge state (to include charge states 2–7) and with monoisotopic precursor selection. Previously interrogated precursors were excluded using a dynamic window (60s ± 10 ppm). The MS2 precursors were isolated with a quadrupole mass filter set to a width of 1.2 m/z. ITMS2 spectra were collected with an AGC target of 10,000, max injection time of 70 ms and CID collision energy of 35%. For FTMS3 analysis, the Orbitrap was operated at 50,000 resolution with an AGC target of 50,000 and a max injection time of 105 ms. Precursors were fragmented by high energy collision dissociation (HCD) at a normalised collision energy of 60% to ensure maximal TMT reporter ion yield. Synchronous precursor selection (SPS) was enabled to include up to five MS2 fragment ions in the FTMS3 scan.

Proteomic data analysis

The raw data files were processed and quantified using Proteome Discoverer software v2.1 (Thermo Scientific) and searched against the UniProt *Staphylococcus aureus* strain NCTC 8325 database using the SEQUEST algorithm [39]. Peptide precursor mass tolerance was set at 10 ppm and MS/MS tolerance was set at 0.6 Da. Search criteria included oxidation of methionine (+ 15.9949) as a variable modification and carbamidomethylation of cysteine (+ 57.0214) and the addition of the TMT mass tag (+ 229.163) to peptide N-termini and lysine as fixed modifications. Searches were performed with full tryptic digestion and a maximum of two missed cleavages were allowed. The reverse database search option was enabled and all peptide data were filtered to satisfy a false discovery rate of 5%.

Statistics

Paired two-tailed student t-test (GraphPad Prism v5.0) were used to analyse the observed differences between experimental results. A *p*-value <0.05 was considered statistically significant. For in vivo studies two-way ANOVA with Tukey post- was used to analyze differences between groups.

References

1. Lowy, F.D. Staphylococcus aureus infections. *N Engl J Med*. 339, 520-32 (1998).
2. Gordon, R.J. & F.D. Lowy, Pathogenesis of methicillin-resistant Staphylococcus aureus infection. *Clin Infect Dis.* **46**, S350-9 (2008).
3.https://assets.publishing.service.gov.uk/government/uploads/system/uploads/attachment_data/file/724361/S_aureus_summary_2018.pdf
4. Jokinen E. et al. Trends in incidence and resistance patterns of Staphylococcus aureus bacteremia. *Infect Dis (Lond).* **50**, 52-58 (2018).
5. Tong S.Y et al. Staphylococcus aureus infections: epidemiology, pathophysiology, clinical manifestations, and management. *Clin Microbiol Rev.* **28**, 603-61 (2015).
6. Seilie, E.S. & Bubeck Wardenburg J. Staphylococcus aureus pore-forming toxins: The interface of pathogen and host complexity. *Semin Cell Dev Biol*. **72**,101-116. (2017).
7. Tam K & Torres VJ. Staphylococcus aureus Secreted Toxins and Extracellular Enzymes. *Microbiol Spectr*. **7**. (2019).
8. Cheung GY, Joo HS, Chatterjee SS & Otto M. Phenol-soluble modulins--critical determinants of staphylococcal virulence. *FEMS Microbiol Rev.* **38**, 698-719 (2014).
9. Wang R et al. Identification of novel cytolytic peptides as key virulence determinants for community-associated MRSA. *Nat Med*. **13**, 1510-4 (2007).
10. Le KY & Otto M. Quorum-sensing regulation in staphylococci-an overview. *Front Microbiol.* **6**,1174 (2015).
11. Bischoff M. et al. Microarray-based analysis of the Staphylococcus aureus sigmaB regulon. *J Bacteriol*. **186**, 4085-99 (2004).
12. Recker M et al., Clonal differences in Staphylococcus aureus bacteraemia-associated mortality. *Nat Microbiol*, **2**, 1381-1388 (2017).
13. Laabei M et al., Predicting the virulence of MRSA from its genome sequence. *Genome Res,* **24**, 839-49 (2014).
14. Laabei M et al., Evolutionary Trade-Offs Underlie the Multi-faceted Virulence of Staphylococcus aureus. *PLoS Biol*, **13**, e1002229 (2015).
15. Diep et al. Complete genome sequence of USA300, an epidemic clone of community-acquired meticillin-resistant Staphylococcus aureus. *Lancet.* **367**, 731-9 (2006).
16. Fey, P.D., et al., A genetic resource for rapid and comprehensive phenotype screening of nonessential Staphylococcus aureus genes. *MBio*, **4**, e00537-12 (2013).
17. Corrigan RM & T. Foster. An improved tetracycline-inducible expression vector for *Staphylococcus aureus*. *Plasmid*. **61**, 126-9 (2009).
18. Horsburgh MJ et al., sigmaB modulates virulence determinant expression and stress resistance: characterization of a functional rsbU strain derived from Staphylococcus aureus 8325-4. *J Bacteriol*. **184**, 5457-67 (2002).
19. Omasits, U et al., Protter: interactive protein feature visualization and integration with experimental proteomic data. *Bioinformatics*. **30**, 884-6 (2014).
20. Liu et al. Staphylococcus aureus golden pigment impairs neutrophil killing and promotes virulence through its antioxidant activity. *J Exp Med*. **202**, 209-15 (2005).
21. Mishra NN et al., Carotenoid-related alteration of cell membrane fluidity impacts Staphylococcus aureus susceptibility to host defense peptides. *Antimicrob Agents Chemother*. **55**, 526-31 (2011).

22. Dayon L & Sanchez JC. Relative protein quantification by MS/MS using the tandem mass tag technology. *Methods Mol Biol.* **893**, 115–127 (2012).
23. Muryoi N et al. Demonstration of the iron-regulated surface determinant (Isd) heme transfer pathway in Staphylococcus aureus. *J Biol Chem*. **283**, 28125-36 (2008).
24. Torrex VJ et al. A Staphylococcus aureus regulatory system that responds to host heme and modulates virulence. *Cell Host Microbe.* **1**, 109-19 (2007).
25. Yeowell HN & White JR. Iron requirement in the bactericidal mechanism of streptonigrin. *Antimicrob Agents Chemother.* **22**, 961-8 (1982).
26. Bullen JJ & Griffiths E. Iron and Infection: Molecular, Physiological and Clinical Aspects. John Wiley and Sons; New York: 1999.
27. Kafala B & Sasarman A. Isolation of the Staphylococcus aureus hemCDBL gene cluster coding for early steps in heme biosynthesis. *Gene*. **199**, 231-9 (1997).
28. Yokoyama et al. Epistasis analysis uncovers hidden antibiotic resistance-associated fitness costs hampering the evolution of MRSA. *Genome Biol*. **19**, 94 (2018).
29. Attia AS, Benson MA, Stauff DL, Torres VJ & Skaar EP. Membrane damage elicits an immunomodulatory program in Staphylococcus aureus. *PLoS Pathog*. 6, e1000802 (2010).
30. Lojek LJ, Farrand AJ, Weiss A & Skaar EP. Fur regulation of Staphylococcus aureus heme oxygenases is required for heme homeostasis. Int J Med Microbiol. 2018 Aug;308(6):582-589.
31. Pozzi C et al. Vaccines for Staphylococcus aureus and Target Populations. *Curr Top Microbiol Immunol*. **409**, 491-528 (2017).
32. Boyle-Vavra S et al. USA300 and USA500 clonal lineages of Staphylococcus aureus do not produce a capsular polysaccharide due to conserved mutations in the cap5 locus. *MBio*. **6**(2) (2015).

22. Allen, R.C., et al., Targeting virulence: can we make evolution-proof drugs? Nat Rev Microbiol, 2014. 12(4): p. 300-8.
23. Gray, B., P. Hall, and H. Gresham, Targeting agr- and agr-Like quorum sensing systems for development of common therapeutics to treat multiple gram-positive bacterial infections. Sensors (Basel), 2013. 13(4): p. 5130-66.
24. Fowler, V.G., Jr., et al., Persistent bacteremia due to methicillin-resistant Staphylococcus aureus infection is associated with agr dysfunction and low-level in vitro resistance to thrombin-induced platelet microbicidal protein. J Infect Dis, 2004. 190(6): p. 1140-9.
25. Rose, H.R., et al., Cytotoxic Virulence Predicts Mortality in Nosocomial Pneumonia Due to Methicillin-Resistant Staphylococcus aureus. J Infect Dis, 2015. 211(12): p. 1862-74.
26. Neumann, Y., et al., The effect of skin fatty acids on Staphylococcus aureus. Arch Microbiol, 2015. 197(2): p. 245-67.
29. Moormeier, D.E., et al., Use of microfluidic technology to analyze gene expression during Staphylococcus aureus biofilm formation reveals distinct physiological niches. Appl Environ Microbiol, 2013. 79(11): p. 3413-24.

27. Tiwari, K.B., C. Gatto, and B.J. Wilkinson, Interrelationships between Fatty Acid Composition, Staphyloxanthin Content, Fluidity, and Carbon Flow in the Staphylococcus aureus Membrane. Molecules, 2018. 23(5).
28. Perez-Lopez, M.I., et al., Variations in carotenoid content and acyl chain composition in exponential, stationary and biofilm states of Staphylococcus aureus, and their influence on membrane biophysical properties. Biochim Biophys Acta Biomembr, 2019. 1861(5): p. 978-987.

Supplementary Material

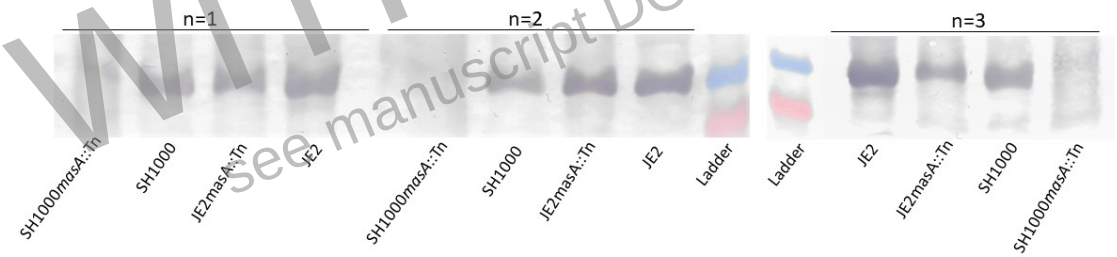

Supplementary Figure 1: The effect of *masA* deletion on alpha toxin secretion was determined by western blotting using anti-alpha toxin antibodies. These blots were scanned, the relative quantity of alpha toxin quantified using ImageJ and these data presented in Figure 1E). Blots from three independent experiments are shown.

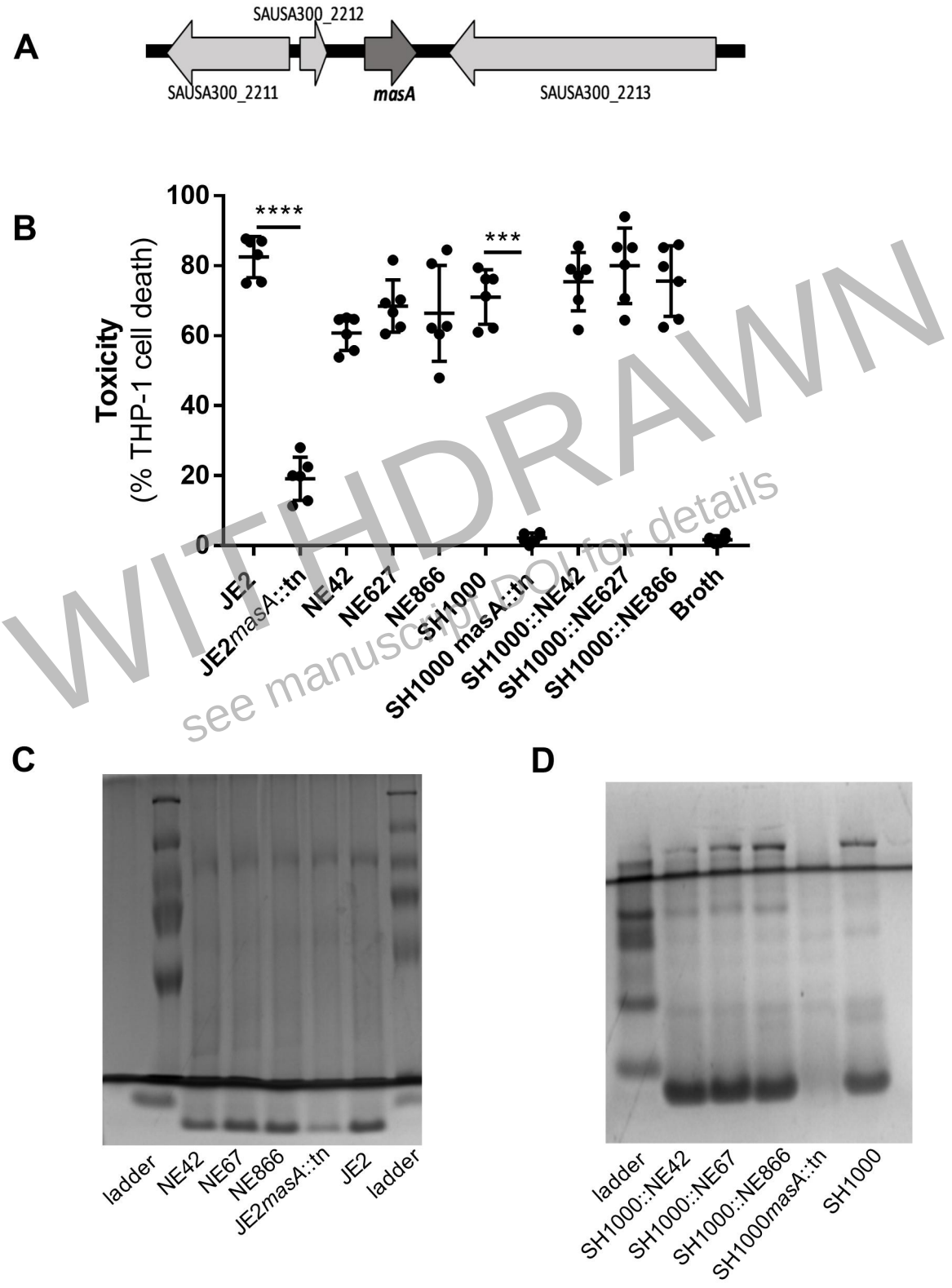

Supplementary Figure 2: (A) A schematic showing the *masA* locus with masA shown in dark grey and neighboring genes shown in light grey. (**B**) The toxicities of transposon mutants of *masA*-neighboring genes in both JE2 and SH1000 backgrounds were tested. NE42 showed a reduced toxicity compared to JE2, but a higher toxicity compared to JE2*masA*::tn. In the SH1000 background, toxicities of these transposon mutants were similar to SH1000 wild type.

848 Representative gels are shown of TCA extractions of PSMs from transposon mutants in the
849 *masA* locus the JE2 **(C)** and SH1000 **(D)** backgrounds.
850

851

852

853

854 **Supplementary Table 1:**

Accession	Functional Description	Fold change	*p*-Value
Q2FVR0	Hemin transport system permease protein HrtB	18.0 ↑	< 0.0001
Q2G079	Protein NrdI	5.8 ↑	0.002
Q2G2P2	Globin domain protein	3.6 ↑	0.001
Q2FUQ9	Cold shock protein	3.5 ↑	0.027
Q2FX98	Uncharacterized protein	3.2 ↑	0.003
Q2FZX4	Lipoyl synthase	2.7 ↑	< 0.0001
Q2FVR1	Hemin import ATP-binding protein HrtA	2.7 ↑	0.006
Q2G0T9	Alpha amylase family protein	2.7 ↑	0.003
Q2FXF4	Uncharacterized protein	2.7 ↑	0.037
Q2FZA9	Carbamate kinase 1	2.6 ↑	< 0.0001
Q8KQR1	Iron-regulated surface determinant protein C	2.6 ↑	0.002
P72360	Iron-sulfur cluster repair protein ScdA	2.6 ↑	0.006
Q2G1N4	Periplasmic binding protein	2.5 ↑	0.008
Q2G1X0	Alpha-hemolysin	2.4 ↑	0.008
Q2FWY2	Pyrazinamidase/nicotinamidase	2.4 ↑	0.029
Q2FV74	ATP-dependent Clp protease ATP-binding subunit ClpL	2.4 ↑	0.001
Q2G2R5	PTS system lactose-specific IIA component	2.3 ↑	0.003
Q2FW75	ABC transporter periplasmic binding protein	2.3 ↑	0.002
Q2FVE7	Peptide ABC transporter, peptide-binding protein	2.3 ↑	0.004
Q2FWB7	Uncharacterized protein	2.2 ↑	0.021
Q2FYK3	Conserved virulence factor C	2.2 ↑	0.004
Q2FXE1	Uncharacterized protein	2.2 ↑	0.007
Q2FZB0	Ornithine carbamoyltransferase	2.2 ↑	< 0.0001
Q2FZJ9	Probable quinol oxidase subunit 2	2.2 ↑	0.006
Q2FVF9	Uncharacterized protein	2.1 ↑	0.034
Q2FV17	Fructose-bisphosphate aldolase class 1	2.1 ↑	< 0.0001
Q2FZF0	Iron-regulated surface determinant protein B	2.1 ↑	0.080
Q2G1Z3	Iron compound ABC transporter	2.1 ↑	0.002
Q2FYN6	Uncharacterized hydrolase	2.0 ↓	0.155
Q2G0L5	Serine-aspartate repeat-containing protein C	2.0 ↓	0.001
Q2G0W6	Uncharacterized protein	2.1 ↓	0.006
Q2FUU5	Lipase 1	2.1 ↓	0.002
Q2FWZ8	Bacterial non-heme ferritin	2.1 ↓	0.001
Q2G294	Acetyl-CoA synthetase	2.1 ↓	0.001
Q2FZI6	Bifunctional purine biosynthesis protein PurH	2.2 ↓	< 0.0001
Q2FVS2	Uncharacterized protein	2.2 ↓	0.001
Q2G2P7	Histidine ammonia-lyase	2.2 ↓	0.006
Q2FW51	Truncated MHC class II analog protein	2.2 ↓	0.015
Q2FVQ4	L-lactate permease	2.2 ↓	0.006

Q2FV59	Dehydrosqualene synthase	2.2	↓	0.001
Q2FUX7	Arginine deiminase	2.3	↓	0.080
Q2FVE0	Alkyl hydroperoxide reductase AhpD	2.3	↓	< 0.0001
Q2G1C7	Uncharacterized protein	2.3	↓	0.006
Q2FZR3	Oligopeptide ABC transporter	2.3	↓	0.004
Q2FZS2	Truncated MHC class II analog protein	2.4	↓	0.004
Q2G0W8	Uncharacterized protein	2.4	↓	0.008
Q2G2P5	Uncharacterized protein	2.4	↓	0.008
Q2FV34	Uncharacterized protein	2.5	↓	0.001
Q2G118	Chromosome partioning protein, ParB family	2.5	↓	0.005
Q2G1I8	Uncharacterized protein	2.5	↓	0.001
Q2FZS8	Chaperone protein ClpB	2.5	↓	0.001
Q2G087	Histidinol-phosphate aminotransferase	2.6	↓	0.047
Q2G1C9	Uncharacterized protein	2.6	↓	< 0.0001
Q2G0G1	Alcohol dehydrogenase	2.8	↓	0.017
Q2FWN9	Uncharacterized leukocidin-like protein 2	2.9	↓	< 0.0001
Q2G1C8	Uncharacterized protein	3.0	↓	< 0.0001
Q2G1D0	Acetyl-CoA acetyltransferase	4.4	↓	0.003
Q2G1K9	Aldehyde-alcohol dehydrogenase	4.6	↓	0.001
Q2FWP0	Uncharacterized leukocidin-like protein 1	4.9	↓	0.003
Q2FVJ5	ATP-dependent dethiobiotin synthetase BioD	6.3	↓	0.001
Q2G218	L-lactate dehydrogenase 1	7.3	↓	0.001
Q2G091	ABC transporter	9.4	↓	< 0.0001
Q2FVJ7	Biotin synthase	9.7	↓	0.001

[#]Accession corresponds to protein identifier in UniProt database.

[€]Fold change of proteins were determined by comparing changes between JE2 and JE2*masA*::tn protein abundances in three independent experiments.

**p*-Value was calculated using the Student's *t*-test

A

Strain	ZoC Area (mm)[#]	*p*-Value*
JE2	4.95 ± 0.28	
JE2 *masA* ::tn	6.58 ± 1.52	<0.0001
JE2 + hemin	6.09 ± 2.26	0.0006
SH1000	5.05 ± 1.31	
SH1000 *masA* ::tn	6.69 ± 2.01	<0.0001
SH1000 + hemin	6.93 ± 3.44	0.001

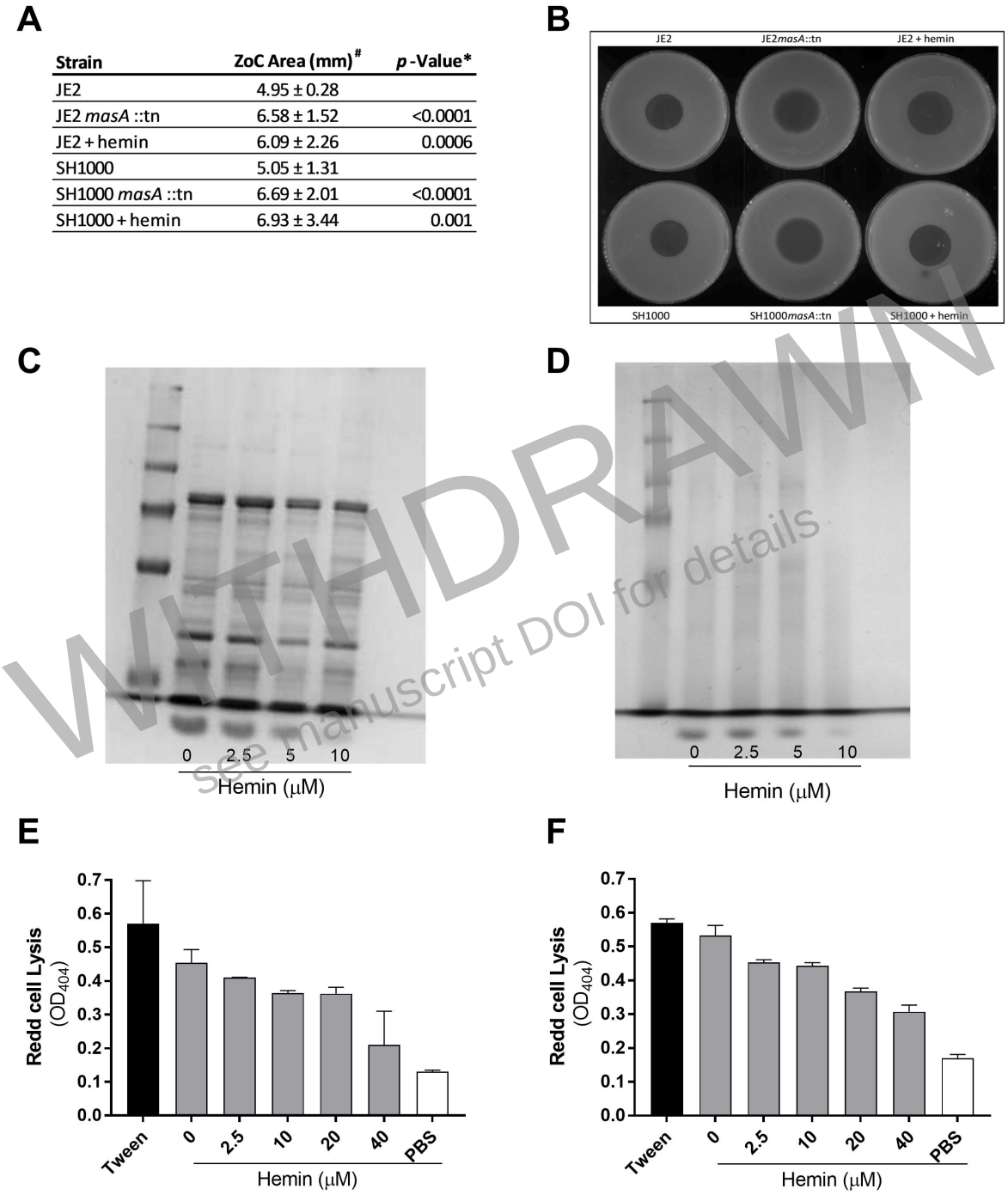

Supplementary Figure 3: (**A**) Ability of streptonigrin to inhibit growth of bacteria was determined via measurement of zone of clearance (ZoC) around 2mg/ml streptonigrin. Greater inhibition of growth occurs for *masA* mutants cultured in TSB and wild types cultured in hemin compared to wild type cultured in TSB. (**B**) Images show representative pictures of the zones of clearance with the following ZoC area in mm: JE2 6.15; JE2*masA*::Tn 9.07; JE2 + 50 μM hemin 8.5; SH1000 5.7; SH1000masA::Tn 8.04; SH1000 + 50 μM hemin 7.06. JE2 (**C**) and SH1000 (**D**) were cultured in various concentrations of hemin and toxins were subsequently TCA precipitated from the supernatants and run on 10% agarose gels. PSM band intensity decreases with increasing hemin concentration. Ability of JE2 (**E**) and SH1000 (**F**) to lyse human red blood cells decreased with increasing hemin concentrations.

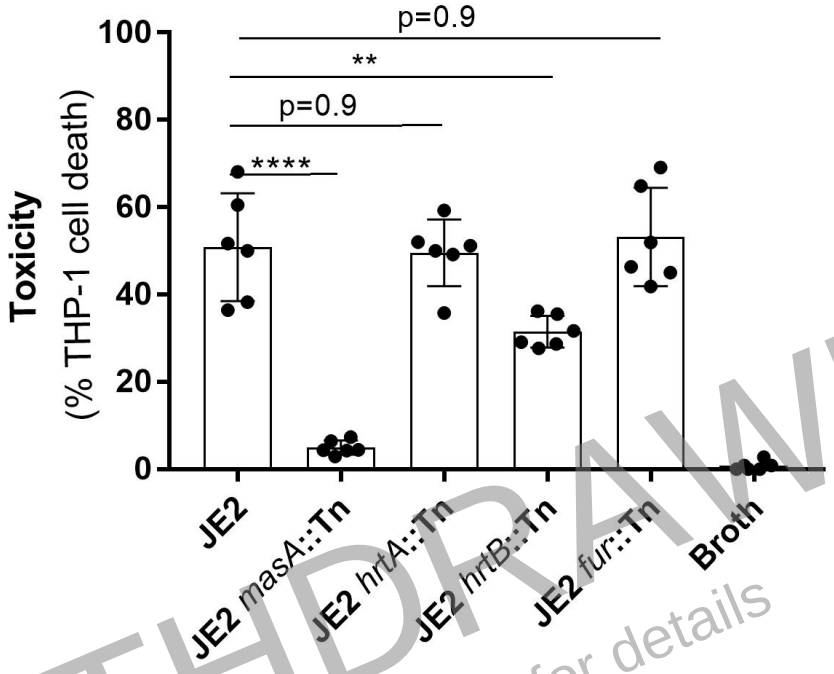

Supplementary Figure 4: The toxicities of transposon mutants of *hrtA* and *hrtB* genes in the JE2 background were tested. JE2*hrtA*::Tn showed no difference in toxicity compared to JE2, while JE2*hrtB*::Tn showed a slightly reduced toxicity, however this was not as dramatic a loss of toxicity as observed in the JE2*masA*::tn strain.